Inter-Research Science Publisher

Aquaculture Environment Interactions
Volume 17:45–57

Published March 6, 2025
https://doi.org/10.3354/aei00490



# Effects of organic particle deposition on porewater oxygenation and oxygen exchange in cohesive sediment

**Michelle N. Simone[1,2,*], Aaron Hibberd[2,3], David Plew[1,4], Kay Vopel[1]**

[1]School of Science, Auckland University of Technology, Auckland 1010, New Zealand
[2]Blue Economy Cooperative Research Centre, Launceston, Tasmania 7250, Australia
[3]Institute for Marine and Antarctic Studies, University of Tasmania, Hobart, Tasmania 7004, Australia
[4]National Institute of Water and Atmosphere, Christchurch 8011, New Zealand

ABSTRACT: This *ex situ* study utilised oxygen microprofiling and whole-core incubations to investigate potential changes in oxygenation of cohesive sediments resulting from open-ocean fin-fish farming. We examined oxygen conditions in sediments subjected to potential moderate depositional loads (1.1, 2.2, and 3.2 g C $m^{-2}$ $d^{-1}$) of organic farm particles from mariculture expected to settle in dispersive environments. White biofilms formed over particulates that accumulated on the sediment surface after 7 d of at least 2.2 g C $m^{-2}$ $d^{-1}$. Diffusive oxygen uptake (DOU) rates were estimated from sediment microprofiles taken in cores following total oxygen uptake (TOU) determination from whole-core incubations. DOU closely aligned with TOU (DOU:TOU ≈ 1) in cores where biofilms did not develop on the sediment surface (<1.1 g C $m^{-2}$ $d^{-1}$); however, the development of biofilms reduced the DOU:TOU ratio (<1), suggesting the biofilms were responsible for non-diffusive oxygen transport in the TOU. It was speculated that 'vents' in the biofilms may have enhanced the solute exchange rates in those cores. The presence of biofilms enhanced benthic TOU, reducing oxygen penetration depths in sediments adjacent to the biofilms by approximately 1 mm compared to unenriched cores. However, these sediments adjacent to biofilms still had an average oxygen penetration of ~2.5 mm, suggesting the patchy accumulation of organic farm particles and development of biofilms on the sediment surface are enhancing the structural heterogeneity of the seafloor and increasing the availability of organic carbon for higher trophic consumers in an otherwise organically deplete system.

KEY WORDS: Sediment oxygenation · Organic deposition · Sediment microprofiling · Biofilm development · Aquaculture

## 1. INTRODUCTION

Since the commercialisation of inshore fin-fish aquaculture, considerable attention has focused on its benthic impacts. Most marine aquaculture, typically situated in sheltered inshore locations, face spatial and environmental constraints, especially regarding the benthic capacity to assimilate or remineralise the settling organic particulates. Operations in low dispersive and/or shallow waters can result in the accumulation of organic particles beneath cages, leading to a shift from predominantly aerobic to anaerobic sediment surfaces (Holmer et al. 2005, Valdemarsen et al. 2012).

White biofilms forming on sediment surfaces beneath aquaculture farms have been used as indicators of dominantly anaerobic benthic conditions (Hamoutene et al. 2016, Simone & Grant 2020). These col-

*Corresponding author: mnhsimone@gmail.com



Publisher: Inter-Research · www.int-res.com

ourless bacteria, appearing white due to accumulated elemental sulfur, exhibit versatile metabolic oxidation strategies. Specifically, these bacteria are capable of aerobic oxidation with dissolved oxygen (Jørgensen 1982) and, in some cases, demonstrate the capacity for anaerobic oxidation, utilising internal stores of nitrate (Fossing et al. 1995, Sayama et al. 2005), underscoring their ecological plasticity (Glud et al. 1998).

In biofilms, mobile *Thiovulum*, *Thioploca*, and *Beggiatoa*-type species eventually dominate sediment surfaces (Bernard & Fenchel 1995, Fenchel & Glud 1998), utilising the reduction–oxidation gradient to orient themselves at the oxic–sulfidic boundary (Nelson et al. 1986b, Preisler et al. 2007). These bacteria efficiently utilise oxygen (Jørgensen 1982), with their formation of biofilms on sediment surfaces associated with an increased potential for benthic diffusive oxygen uptake (DOU) (Nelson et al. 1986a, Jørgensen & Des Marais 1990). Additionally, biofilms can accelerate the exchange of reduced solutes from below their covered area with relatively oxygen-rich overlying waters through vent-like structures that form in the biofilms themselves (Fenchel & Glud 1998, Glud et al. 2004). This accelerated solute exchange mechanism is thought to be generated by the microbial community to increase the supply of oxygen to the bacteria for respiration and reoxidation by ~40 times the supply that would be available from diffusion alone (Fenchel & Glud 1998). As such, the efficient use of oxygen by biofilm-covered sediments can expedite the shift from dominantly aerobic to dominantly anaerobic sediment systems and serve as a proxy for reduced sediment oxygenation around aquaculture sites (Hamoutene et al. 2016, Simone & Grant 2020).

Open-ocean aquaculture, situated in more energetic environments, introduces new potential for organic particles to be dispersed over a larger area. This dispersion of organic material would result in a less concentrated settled footprint compared to less energetic or shallow locations (Valdemarsen et al. 2015). In dispersive environments, organic particles are expected to break apart in the water column, with reaggregation and settlement dictated by the local physical environment. Here, we assess the potential impact of what has been previously defined as 'moderate, detectable enrichment' from dispersive aquaculture sites (~0.8 g C $m^{-2}$ $d^{-1}$; Keeley et al. 2013) to gain a unique perspective on how cohesive sediment, a predominant substrate in deeper waters, may undergo changes in oxygenation. To quantify this potential impact, we injected fresh organic fish waste (faeces, scales, and excess feed) onto organically deplete sediment cores daily for 7 d, targeting 3 levels of moderate enrichment: 1.1, 2.2, and 3.2 g C $m^{-2}$ $d^{-1}$. We employed both oxygen microprofiling and whole-core incubations to measure and compare rates of diffusive and total oxygen uptake (TOU), respectively. Moreover, the use of microprofiling allowed us to define the changes to oxygen penetration in sediments surrounding organic farm waste deposits, which highlighted the potential for increased structural and biogeochemical heterogeneity after 1 wk of moderate organic deposition.

## 2. MATERIALS AND METHODS

For this study, we utilised naturally organically deplete sediments (~0.8% organic carbon) from a subtidal site 47 ± 3 m (mean ± SD) below mean sea level in the temperate Hauraki Gulf, New Zealand (at approximately 36.329° S, 175.182° E). The sediment at this site consisted of cohesive muddy-sand (>50% sand, <50% mud; Folk 1954), with bottom water temperatures ranging from 19.6 to 20.0°C and a mean salinity of 35.47 ± 0.003 determined from 48 h deployments of 2 RBRconcerto$^3$ CTDs moored ~1 m above the sediment surface. Sediment was collected using a KC Denmark multicorer on 22 and 23 February 2022 in 30 acrylic tubes (9 cm diameter × 30 cm length). Each tube contained approximately 23.2 ± 0.4 cm of sediment. Surface sediments (0–2 cm) had a bulk porosity of 0.71. The cores were stored at ~4°C until 27 February, when they were submerged at *in situ* bottom water conditions in a flow-through holding tank at the NIWA Northland Marine Research Centre, Ruakākā, New Zealand.

Cores were inspected for 1 wk before the experiment to identify any large burrows or artefacts of large fauna. If accessible, identified fauna were removed; if they could not be removed, the cores were excluded. This selection of 'undisturbed' cores reduced the non-treatment variability among cores.

All cores were then transferred to large flow-through holding tanks (1500 × 600 × 600 mm; 500 l), with water supplied from a larger header tank (2000 l). The header tank was fitted with multiple chiller units (HC Chiller 300A, Hailea) to bring the ambient temperature down to *in situ* temperatures (~20°C). The flow-through system allowed for full volume turnover every 1.5–2 h. Cores acclimated in the holding tanks for at least 10 d. This acclimation period did not affect organic carbon content in the surface sediment (0–2 cm), remaining at 0.8 ± 0.1% (of dry wt), mimicking

unenriched sediments offshore New Zealand (0.58–1.19% dry wt; Brackley et al. 2010).

### 2.1. Treatments

Following acclimation, we randomly assigned cores (n = 6) to either a control or depositional group. For the depositional groups, 3 levels of enrichment at approximately 1.1, 2.2, or 3.2 g C $m^{-2}$ $d^{-1}$ were chosen to represent increasing enrichment levels based on detectable or moderate depositional estimates from fin-fish farms in dispersive waters in Keeley et al. (2013) (~0.8 g C $m^{-2}$ $d^{-1}$). To ensure a comprehensive assessment, both a positive control (~11.2 g C $m^{-2}$ $d^{-1}$) and negative control (no added organic material) were employed. This procedure aimed to verify that the sediments selected were responsive to organic enrichment and provide a high-depositional environment (Keeley et al. 2013) and unenriched reference point, respectively.

We extended the flow-through system from the header tanks to 6 tanks (each 400 l and 740 × 1800 mm): 3 treatment tanks, 2 control tanks, and 1 incubation tank. In these tanks, water was upwelled and aerated to maintain water column mixing and ensure oxygen saturation above the sediments.

Over 7 d, fresh fish waste was collected every morning from passive settlement traps attached to a fish tank housing kingfish (~1.9 kg each) at a stocking density of 42.9 kg $m^{-3}$. Settlement traps were flushed and cleaned approximately 3 h prior to waste collection to exclude 'old' waste and excess feed. Following collection, the waste was centrifuged at 2500 rpm (1400 × *g*) for 3 min (Spintron Centrifuges GT-20) and excess water was decanted. Visual inspection of the remaining material verified that the organic waste maintained its structure following centrifuging.

A subsample (~7 g) of daily waste collected was frozen and then freeze-dried prior to elemental analysis of carbon and nitrogen using a CE440 Elemental Analyser (Exeter Analytical). The remaining waste was diluted with seawater (1:1 w/v), mixed well, and then syringe-sampled (0.6 ml) into 2 clean containers. These samples were placed into a 50°C oven for 48 h and then measured for dry weight to calculate the water content of the 'injected' waste (89 ± 1%, n = 22). Subsequently, the dry waste was combusted at 490°C to determine organic matter content (72 ± 7%). The remaining diluted waste was used to enrich sediment cores.

The sediment cores received daily injections of 0.2, 0.4, 0.6, or 2 g, corresponding to 3 enrichment levels considered in a moderate depositional range and the positive control: ~1.1, 2.2, 3.2, and 11.2 g C $m^{-2}$ $d^{-1}$, respectively. Dilute fish waste was injected with a syringe into undisturbed (no bubbling) water columns immediately above sediment surfaces, allowing approximately 1 h for the waste to settle on the sediment surface before reintroducing water column mixing.

### 2.2. Sediment core incubations

Following the seventh waste injection, and approximately 20 h after water column mixing resumed, each core was sealed with a custom-fit lid that had an inlet and outlet port to facilitate water column circulation during incubations. Water was circulated through polyetheretherketone (PEEK) tubes using a peristaltic pump (25 rpm, Kamoer FX-STP WiFi reef aquarium dosing peristaltic pump), ensuring thorough mixing of the water columns while not disturbing the sediment surface. An in-line optical sensor (PreSens Precision Sensing) was used in one core from each treatment to monitor oxygen concentration during the incubation period. This allowed for incubations to be terminated before water column oxygen concentrations dropped below ~80% air saturation. Oxygen concentrations in all cores were measured using an oxygen dipping probe (PM-PSt7, PreSens Precision Sensing) at the beginning and end of each incubation, enabling the calculation of TOU (μmol $m^{-2}$ $h^{-1}$).

### 2.3. Sediment properties

We took sediment surface photographs after 1 d and after 7 d of enrichment to quantify visual changes over time. Following the determination of TOU, we sacrificed 3 of the 6 sediment cores to measure the organic carbon content of the surface sediment (0–2 cm). The sediment samples were freeze-dried and subsequentially subsampled, weighed, acidified (0.1 M HCl; Kennedy et al. 2005), and dried again for elemental analysis (CE440 Elemental Analyser, Exeter Analytical). The 3 remaining sediment cores in each depositional group were left uncapped in the holding tanks until microprofiling.

### 2.4. Microprofiling and consumption rates

We haphazardly measured 5 vertical porewater oxygen concentration microprofiles in each core with an oxygen microsensor (PM-PSt-7, PreSens Preci-

sion) on a micromanipulator. For cores that developed white biofilms, we measured up to 5 microprofiles in biofilm-covered areas in addition to the 5 microprofiles in 'uncovered' sediments. Note that microprofiles measured in biofilms avoided vent-like structures to characterise the diffusive flux across the biofilm and to avoid potential convective currents generated by the vent and edge structures (Fenchel & Glud 1998, Glud et al. 2004). Similarly, microprofiles in uncovered sediments were measured in areas free of faunal traces (i.e. discarded tube casts or shell deposits) to best characterise the dominant surface type.

To maintain advection and ensure proper mixing of the seawater overlying the sediment core without resuspending sediment particles, we used a small tube and a peristaltic pump to drip seawater, pumped from the main incubation tank, onto the surface of the sediment core-overlying seawater. The shape of the measured oxygen concentration microprofiles, along with visual inspection of the seawater column, confirmed that this approach provided sufficient mixing without disturbance of the sediment.

Oxygen concentrations were measured at 200 µm intervals, starting approximately 2–4 mm above the sediment–water interface and continuing to a depth where oxygen concentrations dropped below 1 µmol $l^{-1}$. We defined the oxygen penetration depth (OPD) on each microprofile as the depth at which oxygen concentrations fell below 4.5 µmol $l^{-1}$ (Table 1).

We used microprofiles to derive the diffusive flux across the sediment–water interface and to compute the depth-resolved volumetric consumption rates ($R_V$), using the PROFILE model (Berg et al. 1998). All PROFILE inputs and computation notes are detailed in Table 2 (for full model details see Text S1, Table S1 and Figs. S1–S3 in the Supplement at www.int-res.com/articles/suppl/q017p045_supp.pdf). The total DOU for each core was determined as the mean of the depth integrated $R_V$ values computed from each microprofile. In cores where both biofilm-covered and un-

Table 1. Summary of total oxygen uptake (TOU) rates measured from sealed core incubations and diffusive oxygen uptake (DOU) rates computed from microprofiles (µmol $m^{-2}$ $h^{-1}$). Mean (±SE) DOU rates are presented for biofilm-covered and uncovered areas, with the biofilm cover (%) used to calculate the mean (±SE) net DOU rate for each core. The DOU/TOU ratio describes the relationship between oxygen uptake measurements, with values closest to 1 indicating the greatest similarity. Differences in uptake rates were considered significant when the proportional difference between TOU and DOU (TOU − DOU) in TOU exceeded 2.78 (95% CI), based on the proportion of the DOU standard error (DOU_SE) in TOU determined significantly different uptake rates if the proportional difference of TOU to DOU (TOU − DOU) in TOU was greater than 2.78 (95% CI). Asterisks indicate cores where the proportional difference between measurements was $^{\star}\geqslant 2.78$ up to 3.77, $^{\star\star}\geqslant 3.78$ up to 4.77 and $^{\star\star\star}\geqslant 4.78$ SEs. Mean (±SD) oxygen penetration depth (OPD) below the sediment–water interface and the surface of biofilms (Biofilm) were calculated from microprofiles in uncovered and covered sediments, respectively. Pos Con: positive control

| Treatment | TOU | Biofilm (%) | DOU (±SE)[a] Covered | Uncovered | Net | $\left(\frac{DOU}{TOU}\right)$ | $\left(\frac{DOU\_SE}{TOU}\right)$ | $\left(\frac{TOU-DOU}{TOU}\right)$ | OPD (mm) | Biofilm (mm) |
|---|---|---|---|---|---|---|---|---|---|---|
| Control | 296 | 0 | 0 | 289 (±17) | 289 (±17) | 0.98 | 0.06 | 0.02 | 3.68 (±0.18) | – |
| Control | 245 | 0 | 0 | 272 (±17) | 272 (±17) | 1.11 | 0.07 | −0.11 | 3.88 (±0.33) | – |
| Control | | | | 389 (±47) | 389 (±47) | | | | 3.28 (±0.41) | – |
| Low | 632 | 0 | 0 | 666 (±45) | 666 (±45) | 1.05 | 0.07 | −0.05 | 2.64 (±0.22) | – |
| Low | 760 | 0 | 0 | 679 (±41) | 679 (±41) | 0.89 | 0.05 | 0.11 | 2.60 (±0.57) | – |
| Low | 583 | 0 | 0 | 542 (±34) | 542 (±34) | 0.93 | 0.06 | 0.06 | 3.56 (±0.22) | – |
| Mid | 637 | 0 | 0 | 519 (±42) | 519 (±42) | 0.82 | 0.07 | 0.18$^{\star}$ | 2.92 (±0.64) | – |
| Mid | 573 | 3 | 1747[c] | 447 (±21) | 488 (±20) | 0.85 | 0.04 | 0.15$^{\star\star}$ | 2.80 (±0.58) | 0.4[c] |
| Mid | 680 | 0 | 0 | 642 (±83) | 642 (±83) | 0.94 | 0.12 | 0.06 | 2.40 (±0.58) | – |
| High | 1111 | 27 | 908 (±75) | 546 (±47) | 644 (±40) | 0.58 | 0.04 | 0.39$^{\star\star\star}$ | 2.16 (±0.43) | 1.7 (±0.5) |
| High | 947[b] | 21 | 1025 (±56) | 698 (±50) | 767 (±41) | 0.81 | 0.04 | 0.18$^{\star\star}$ | 2.24 (±0.43) | 1.6 (±0.3) |
| High | 835 | 24 | 905 (±42) | 641 (±42) | 705 (±34) | 0.84 | 0.04 | 0.19$^{\star\star}$ | 2.16 (±0.43) | 2.0 (±0.4) |
| Pos Con | 2011 | 76 | 1544 (±48) | 346 (±28) | 1255 (±37) | 0.62 | 0.02 | 0.36$^{\star\star\star}$ | 3.12 (±0.54) | 1.2 (±0.31) |
| Pos Con | 1328 | 100 | 1048 (±69) | 0 | 1048 (±69) | 0.79 | 0.05 | 0.22$^{\star\star}$ | N/A | 1.4 (±0.2) |
| Pos Con | 1993 | 38 | 1441 (±105) | 485 (±77) | 844 (±62) | 0.42 | 0.03 | 0.50$^{\star\star\star}$ | 2.48 (±0.56) | 1.0 (±0.2) |

[a]Net DOU standard error is approximated as the $\sqrt{(1-p)^2 SE_U + p^2 SE_C}$ where the SE for uncovered ($U$) and biofilm-covered ($C$) sediments are weighted by the estimated proportion of the surface area covered by a biofilm ($p$)

[b]Mean TOU of the other 5 cores (947 ± 110 mmol $m^{-2}$ $h^{-1}$) was used in place of the individual core TOU because the TOU rate of this core (613 mmol $m^{-2}$ $h^{-1}$) was more than 3 standard deviations lower than the other 5 cores. This was likely due to an operator error when recording the final oxygen concentration

[c]Due to the low surface area, only 1 microprofile was measured in the biofilm of this core. As such, the 'covered DOU' and the vertical reach of the 'biofilm (mm)' are estimated from a single microprofile

Table 2. PROFILE model inputs. DBL: diffusive boundary layer; SWI: sediment–water interface; ϕ: porosity (see Supplement for further details)

| Input | Value | Notes | Source |
|---|---|---|---|
| Depth at top of calculation domain | 0 | DBL not included | |
| Depth at bottom of calculation domain | x_max | Final measurement for replicate | Measured |
| Maximum number of equally spaced zones | 10 | | Selected |
| Type of boundary conditions | 4 | Concentration at SWI, zero flux at base | Selected |
| First boundary condition | $C_{SWI}$ | Concentration at SWI | Measured |
| Second boundary condition | 0 | Zero flux at base | Selected |
| Diffusivity in water ($D$) ($cm^2\ s^{-1}$) | $1.957 \times 10^{-5}$ | Free solution at 20.2°C, salinity 35 | Brecker & Peng (1974) |
| Expression for sediment diffusivity ($D_S$) | 2 | $D_S = \phi^2 d$ | Ullman & Aller (1982) |
| Concentration in water column ($C_0$) | N/A | No irrigation[a] | – |
| Minimum for production rate | $-1 \times 10^{20}$ | Nominal large negative | – |
| Maximum for production rate | 0 | Insufficient light | Selected |
| Maximum deviation for acceptance | 0.001 | Default | Berg et al. (1998) |
| Level of significance in the $F$-statistics | 0.01 | Default | |

[a]Irrigation ($\alpha = 0$) and bioturbation ($D_B = 0$) due to removal of macrofauna

covered sediments were present, the DOU was calculated by first estimating the biofilm coverage (%) from surface photographs (Fig. 1) using ImageJ. We manually outlined the mat-covered area of the sediment surface and the circumference of the sediment core to calculate the percent coverage based on the number of pixels enclosed in the 2 outlined areas. The biofilm coverage was then used to weight the mean $R_V$ values calculated in the biofilm-covered and uncovered areas according to their respective surface areas.

We considered a gradient tortuosity correction for the oxygen diffusivity coefficient in uncovered sediments. Specifically, using Archie's law, an 85% surface porosity, which decayed at an exponential depth scale of 1 mm towards the measured bulk porosity (71.4%), was used in the PROFILE model. The sediment surface was identified in each microprofile as an inflection point in the upper region of the concentration gradient, where the diffusivity decreases due to tortuosity (Røy et al. 2004). Similarly, microprofiles measured in bacterial biofilms identified the first inflection point, where the diffusivity decreased due to tortuosity, as the surface of the biofilm. Note that the sediment surface, or base of the biofilm, was not apparent in the microprofiles due to the 200 µm interval scale and low oxygen concentrations obscuring any second inflection. This inability to identify the base of biofilms is unlikely to affect DOU rates, as rates are unaffected by biofilm thickness of >0.2 mm, and in previous studies, thinly veiled to fibrous biofilms ranged from 0.2 to 0.6 mm (Bernard & Fenchel 1995, Fenchel & Bernard 1996). While we expect variation in biofilm density and, consequently, solute diffusivity within the biofilm structure (Wieland et al. 2001), we had assumed a constant porosity of 95% (Bernard & Fenchel 1995) for the biofilm microprofiles in PROFILE.

### 2.5. DOU versus TOU

We compared the DOU to the TOU for each core by examining the proportion of TOU explained by DOU (DOU/TOU). Cores with DOU/TOU values close to 1 indicated that oxygen uptake was predominately driven by molecular diffusion, while values <1 suggested that non-diffusive uptake contributed to the TOU (Glud 2008).

### 2.6. Statistical analysis

We conducted a 1-way ANOVA on the TOU data set to investigate the potential impact of the depositional load (n = 5) on TOU (n = 6) following 7 d of moderate enrichment. The TOU data set did not meet normality assumptions based on the Shapiro-Wilk test; therefore, we applied a log transformation and used $\alpha = 0.01$ to limit the potential for type one error.

Additionally, a 1-way ANOVA was performed on the organic carbon and OPD data set to assess whether the depositional load (n = 5) had a significant effect on the organic carbon content of surface sediments (n = 3) and OPD (n = 3) after 7 d of enrichment.

To further analyse the difference between DOU and TOU, we used the standard errors (SE) on DOU from the treatment and control groups (Table 1). Significance was established when the proportion

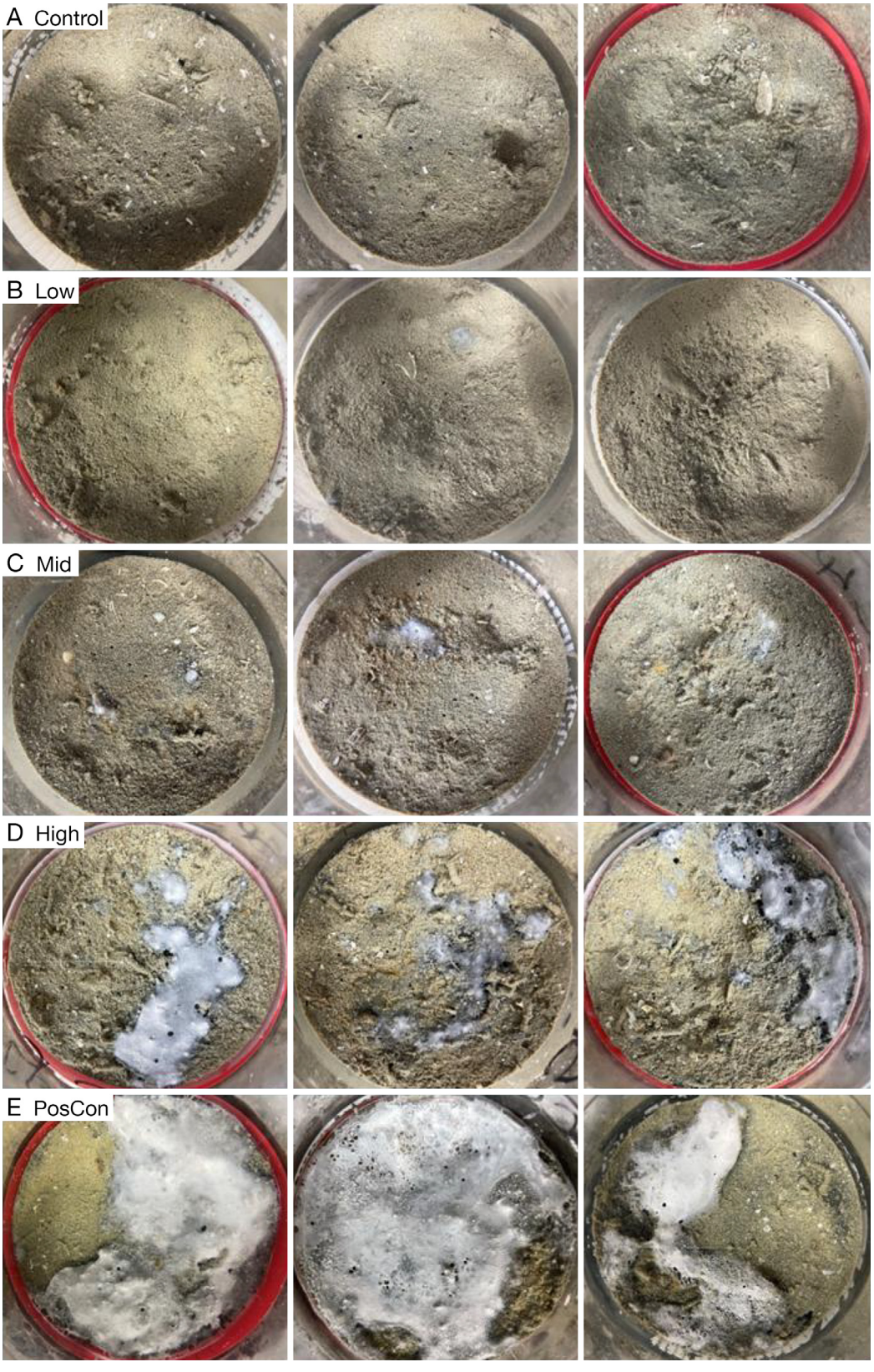


Fig. 1. Surface images of microprofiled sediment cores in the (A) negative control, (B) lowest (1.1 g C $m^{-2}$ $d^{-1}$), (C) mid (2.2 g C $m^{-2}$ $d^{-1}$), and (D) high-moderate (3.2 g C $m^{-2}$ $d^{-1}$) depositional groups, as well as the (E) positive control (11.2 g C $m^{-2}$ $d^{-1}$) group

of TOU explained by the DOU was more than 2.78 SE, corresponding to an approximately 95% confidence interval. All statistical tests were run with R version 4.3.1 (R Core Team 2023), with significance defined at a maximum $\alpha = 0.05$.

## 3. RESULTS

### 3.1. Sediment properties and visual differences

The injected fish waste had a consistent organic matter content of 72 ± 7% (±SD) and carbon content of 29 ± 4%, with a C:N ratio of 11 ± 1 and water content of 89 ± 1%. Organic carbon content of surface sediments increased with increasing depositional load ($F_{4,10} = 4.6$, $p = 0.02$; Fig. 2A), with lowest concentrations measured in the negative control and cores that received the low-moderate depositional load (97 ± 7 and 83 ± 12 g C $m^{-2}$, respectively) and highest concentrations measured in the high-moderate depositional load and positive control cores (123 ± 5 and 115 ± 25 g C $m^{-2}$, respectively).

Photographs taken before and after 7 d of enrichment showed clear visual differences among the depositional groups (Fig. 1). Sediment cores that received waste deposits of at least 2.2 g C $m^{-2}$ $d^{-1}$ developed white biofilms (Table 1). The injection of particulate waste, simulating what is released from the fish, led to patchy accumulations on sediment surfaces. Consequently, the structure and opacity of the biofilms covering these patches also varied both within and among the depositional groups (Fig. 1).

Biofilms displayed a visual range from thinly grey veils to denser or opaque white and fibrous covers with vent-like structures (Fig. 1). For example, a small opaque white patch of ~3% coverage (Fig. 1) was found on one of the 3 cores microprofiled in the mid-depositional group (2.2 g C $m^{-2}$ $d^{-1}$), similar to those observed on two of the 3 sacrificed cores immediately following the TOU incubation (images not shown). In contrast, biofilms on the surface of the cores in the high-moderate depositional group (3.2 g C $m^{-2}$ $d^{-1}$) exhibited opaque to visually thin or veiled covers, covering 20–30% of the core surface. Additionally, these biofilms in the high-moderate depositional group had vent-like structures both within the biofilm and along the edges (Fig. 1). Finally, the positive control cores had the greatest biofilm coverage, covering 35% to almost 100% of the sediment surface in some instances. Vent-like structures were again present within and along the edges of these opaque and fibrous biofilms (Fig. 1).

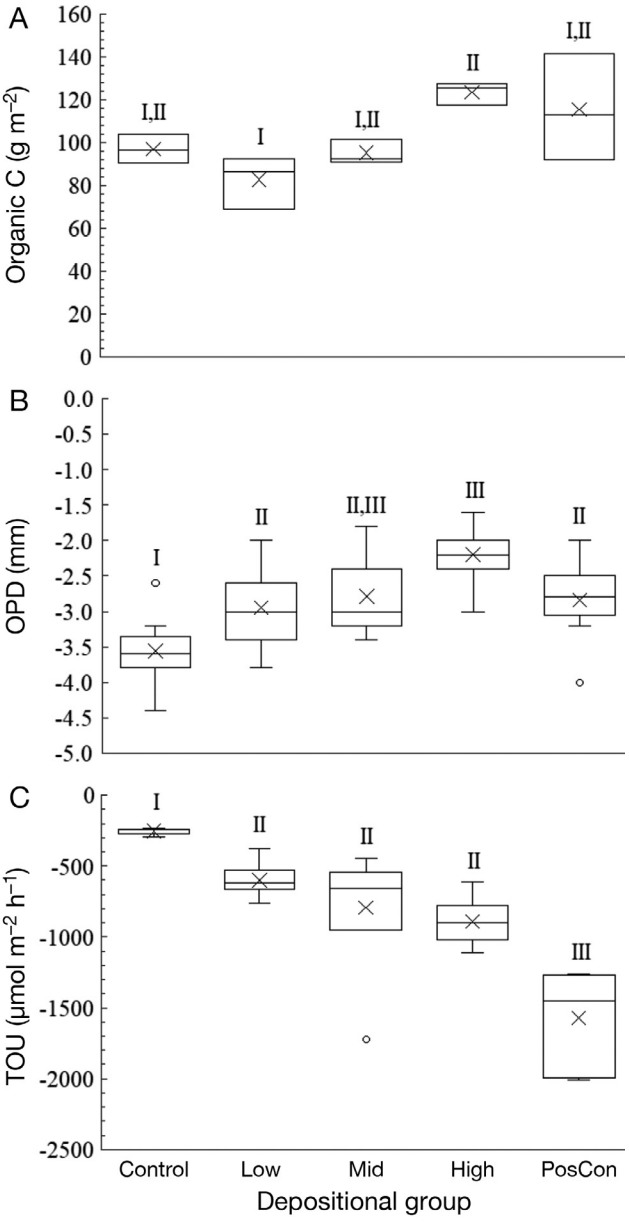


Fig. 2. (A) Organic carbon content measured in surface sediments (0–2 cm), (B) oxygen penetration depth (OPD), and (C) total sediment oxygen uptake (TOU), across moderate depositional loads (from low to high: 1.1, 2.2, and 3.2 g C $m^{-2}$ $d^{-1}$) and controls (0 and positive control [PosCon] 11.2 g C $m^{-2}$ $d^{-1}$) after 7 d of enrichment. In all boxes, '×': mean ( n = 3, 15, and 6 for A, B, and C, respectively); middle horizontal line: exclusive median; top and bottom edges: upper and lower quartiles, respectively. Roman numerals that are the same indicate no significant difference ($\alpha = 0.05$ for A and B, and 0.01 for C)

Due to the small size of the biofilm on the core in the mid-depositional group, only one microprofile was measured instead of the 5 measured in all other biofilms on the surface of cores in the high-moderate depositional and positive control group. Biofilm oxy-

genation varied among depositional groups, ranging from 24 to 52 ± 13% air saturation measured at the surface of visually dense biofilms found on the mid-depositional group (2.2 g C $m^{-2}$ $d^{-1}$) and positive control cores, respectively, and 73 ± 7% air saturation measured at the surface of visually thin and structurally variable biofilms found on the cores in the high-moderate depositional group (3.2 g C $m^{-2}$ $d^{-1}$) (Fig. 3). Oxygen penetration below the biofilm surface also varied with depositional loading, with shallowest penetrations of 0.4 mm measured in the mid-depositional group to the greatest depths of 1.6–2 mm in the high-moderate depositional group (Table 1). The below biofilm oxygen variability was 2.4 times greater in the first 1 mm among the visually variable biofilms measures on the cores that received the high-moderate depositional load (3.2 g C $m^{-2}$ $d^{-1}$) than were measured among the denser and opaque biofilms on the surface of the positive control cores (Fig. 3).

Mean OPDs in uncovered sediments were generally shallower with increasing levels of enrichment ($F_{4,65}$ = 14.5, p < 0.0001; Fig. 2B), ranging from deepest OPDs measured in cores from the negative control and lowest depositional group (3.6 ± 0.4 and 2.9 ± 0.6 mm, respectively) to the shallowest OPDs measured in the core of the high-moderate depositional and positive control groups (2.2 ± 0.4 and 2.8 ± 0.6 mm, respectively).

### 3.2. Sediment oxygen uptake

Increasing depositional load significantly increased TOU ($F_{4,24}$ = 31.32, p < 0.0001), with the lowest TOU measured in the negative control cores (~253 ± 24 µmol $m^{-2}$ $h^{-1}$) and the highest uptake rates measured in the positive control cores (~1572 ± 351 µmol $m^{-2}$ $h^{-1}$; Fig. 2C).

Estimates of DOU matched TOU measurements in cores from the negative control and lowest depositional group (DOU/TOU ≈ 1; 95% CI; Table 1). This agreement between DOU and TOU suggests that molecular diffusion was the main mechanism that drove oxygen exchange for these sediments. In contrast, at higher rates of deposition, where sediments received at least 2.2 g C $m^{-2}$ $d^{-1}$, DOU was consistently less than TOU (Table 1), with diffusive uptake accounting for as little as 42% of TOU in one of the positive control cores. Regardless of depositional load, oxygen microprofiles showed a consistent diffusive boundary layer (DBL) thickness of 0.6–0.8 mm (Fig. 3).

## 4. DISCUSSION

Our experiment suggests that cohesive sediments, naturally deplete in organic matter, may see an increase in oxygen heterogeneity after 1 wk of moderate organic deposition expected from aquaculture operations in dispersive environments. By focusing on what is expected to be a 'detectable' level of loading on sediments in dispersive environments (~0.8 g C $m^{-2}$ $d^{-1}$; Keeley et al. 2013), we were able to assess the changes in sediment oxygen conditions to what will likely be a minimum load of fin-fish farming activities that move offshore, into open and dispersive waters.

The sediments selected for this study had a total organic carbon content of ~0.8% dry wt, well within the range measured in other New Zealand sediments collected from ~60–1430 m depth off the Gisborne District coast in north-eastern New Zealand (0.58–1.19% dry wt; Brackley et al. 2010). However, the calculated rates of TOU (~250 µmol $m^{-2}$ $h^{-1}$) were under the assumed benthic respiration rate of global marine sediments of a similar depth, ~916 µmol $m^{-2}$ $h^{-1}$ ($R = 32.1e^{-0.0077z}$; Middelburg et al. 2005). Our intentional removal of macrofauna from the sediment cores would have undoubtedly contributed to this lower TOU; however, access to labile organic carbon was likely limiting the metabolic potential of the remaining sediment community. While lability was not directly evaluated in this study, the deposition of 1.1 g C $m^{-2}$ $d^{-1}$ on sediments in the lowest depositional group more than doubled the TOU measured in unenriched sediment cores, with no significant increases thereafter between the mid and high-moderate depositional groups, despite adding 2 or 3 times the organic material (Fig. 2C). Moreover, the slight decrease in organic carbon content measured in surface sediments of cores that received the lowest deposits of fresh organic matter built back up in surface sediments of core that received mid-depositional loads and increased thereafter (Fig. 2A), suggesting a potential priming of sediment communities for the use of 'old' or existing organic carbon (Riekenberg et al. 2020). As such, the rate of TOU in naturally organically deplete cohesive sediments will likely increase after a moderate deposit of fresh organic material (1.1–3.2 g C $m^{-2}$ $d^{-1}$).

Visually, sediment surfaces only differed once biofilms developed over organic deposits on cores that received at least 2.2 g C $m^{-2}$ $d^{-1}$; twice the depositional rain that was found to significantly increase the TOU rates (Fig. 2C). While no formal identification of biofilm community structure was run in this study, motile chemolithotrophic sulfur-oxidising bacteria

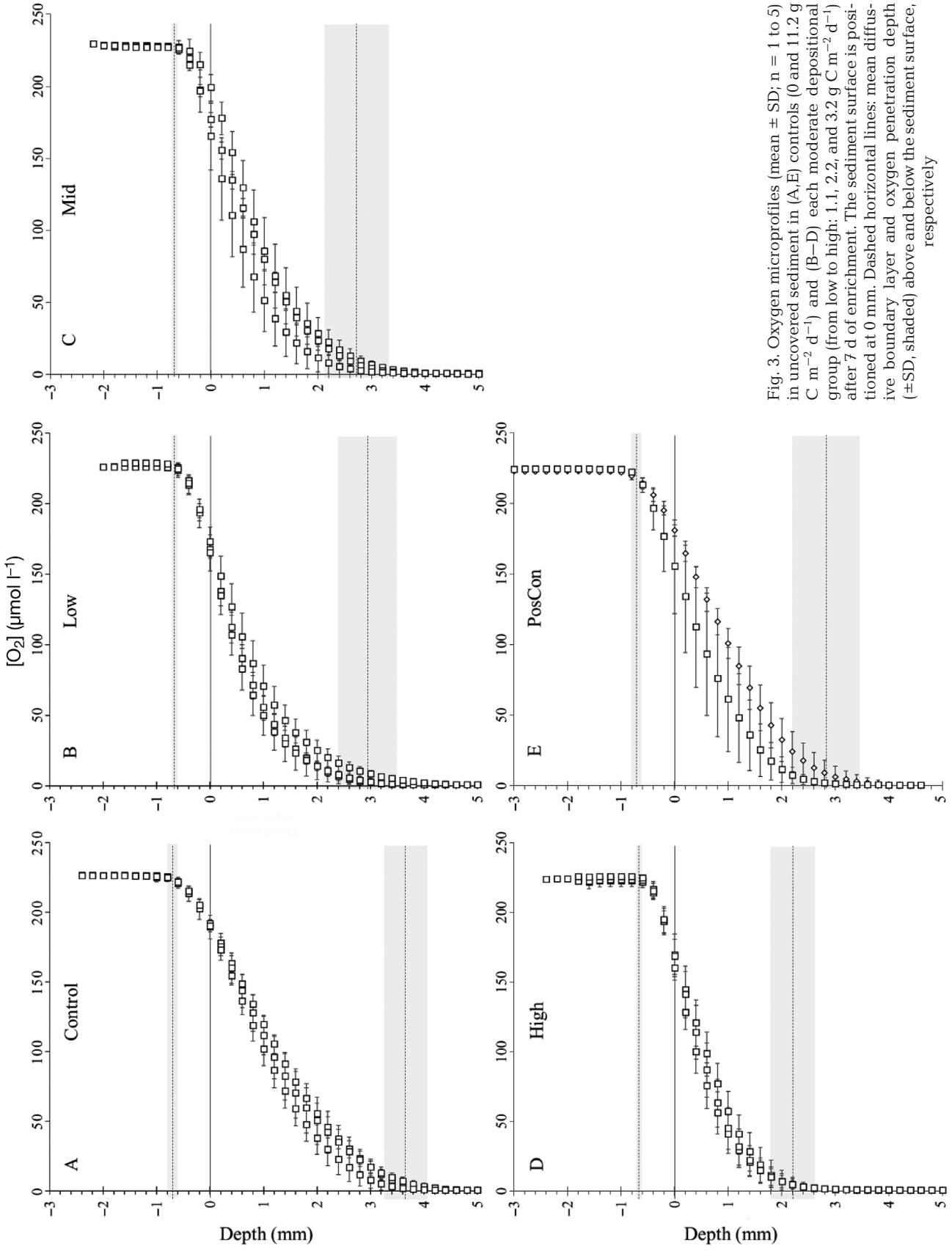


Fig. 3. Oxygen microprofiles (mean ± SD; n = 1 to 5) in uncovered sediment in (A,E) controls (0 and 11.2 g C $m^{-2}$ $d^{-1}$) and (B–D) each moderate depositional group (from low to high: 1.1, 2.2, and 3.2 g C $m^{-2}$ $d^{-1}$) after 7 d of enrichment. The sediment surface is positioned at 0 mm. Dashed horizontal lines: mean diffusive boundary layer and oxygen penetration depth (±SD, shaded) above and below the sediment surface, respectively

are ubiquitous in marine sediments (Dyksma et al. 2016). These biofilms are characterised by a succession of sulfur-oxidising bacteria (Bernard & Fenchel 1995), where the microbial community changes from fast-colonising, free-swimming bacteria that form loose, veil-like biofilms on sediment surfaces within oxygen tensions of 1–20% atmospheric saturation (Fenchel & Bernard 1995) and biofilm thicknesses of ~200 µm (Bernard & Fenchel 1995, Fenchel & Bernard 1996) to stabilising, filamentous, mat-like biofilms that position themselves at oxygen concentrations <5% air saturation (Møller et al. 1985) and have biofilm thickness from 0.5 to >6 mm (Bernard & Fenchel 1995, Glud et al. 2004). While our visually dense and fibrous biofilm that formed on the surface of sediments that received moderate depositions of 2.2 g C $m^{-2}$ $d^{-1}$ fell close to these expected concentrations (<25% air saturation at the surface, dropping below 2% within 0.4 mm), some of the structurally variable biofilm microprofiles in the high-moderate depositional group (3.2 g C $m^{-2}$ $d^{-1}$) had 73 ± 7% air saturation measured at the biofilm surface and only dropped below 2% after 1.6–2 mm (Fig. 4). While potential differences in biofilm succession among cores and depositional groups could help explain why the sometimes visually thin and structurally variable biofilms on the surface of sediments that received 3.2 g C $m^{-2}$ $d^{-1}$ had higher concentrations of oxygen measured, the saturations are still greater than are generally observed in similar biofilms (Fenchel & Bernard 1995).

A possible explanation for the higher than previously described oxygen tensions may be a result of the aerial vertical insertion of the microelectrode compressing the DBL (Glud et al. 1998). This has been observed previously in Glud et al. (1998), where vertically inserted 5 µm microelectrodes introduced ~9% air saturation into biofilms relative to the air saturation measured with planar optodes. Because thicker sensors have a greater potential to affect the free flow of water across the DBL, the robust sensor tip used in this study (230 µm) may have partially contributed to

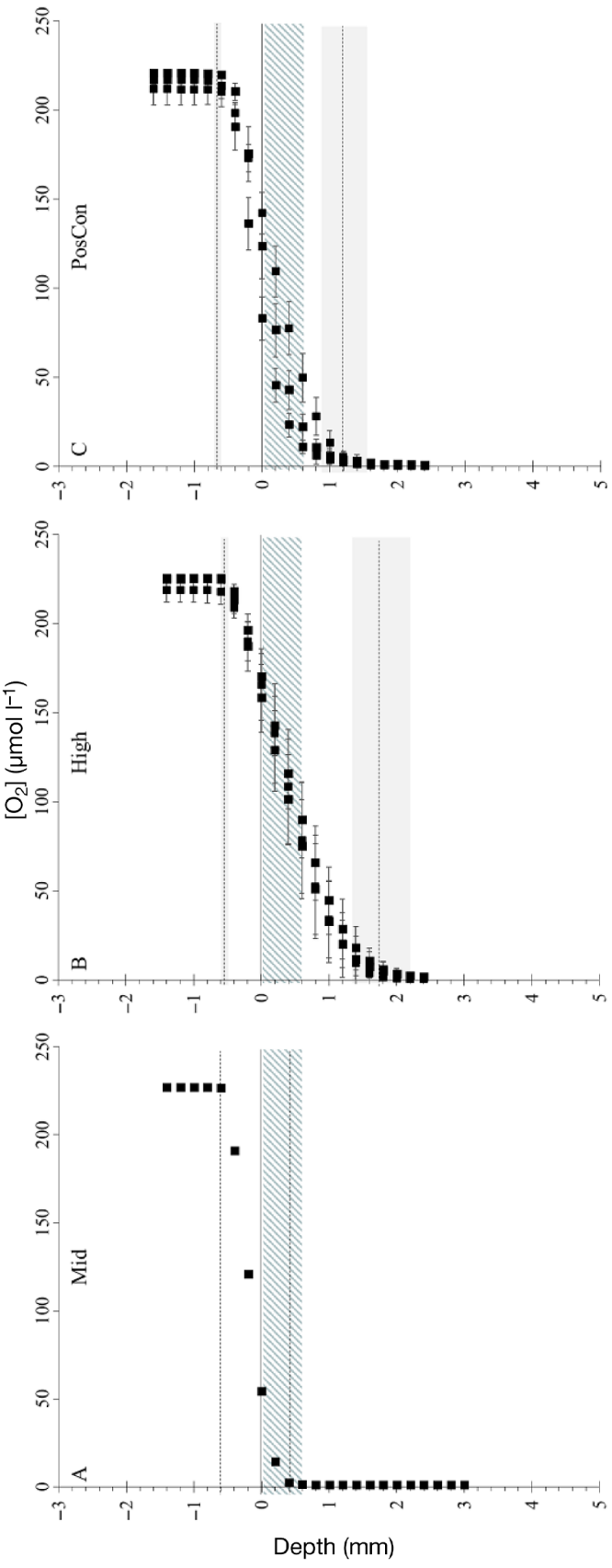


Fig. 4. Oxygen microprofiles (mean ± SD; n = 1 to 5) in biofilm-covered sediment in (A) mid to (B) high moderate depositional groups (2.2 and 3.2 g C $m^{-2}$ $d^{-1}$, respectively) and (C) positive control cores (11.2 g C $m^{-2}$ $d^{-1}$) after 7 d of enrichment. The biofilm surface is positioned at 0 mm. Dashed horizontal lines: mean diffusive boundary layer and oxygen penetration depth (±SD, shaded) above and below the biofilm surface, respectively. Hatch-shaded areas directly below the sediment surface show the potential thickness of the biofilm (Bernard & Fenchel 1995)

the >70% air saturation measured in some biofilms (Fig. 4). However, this was most apparent in structurally variable and occasionally 'thin' biofilms, which also likely had a greater susceptibility for biofilm oxygenation. Despite this potential oxygenation, assuming the filamentous biofilms occupied a 500–600 µm-thick zone (Nelson et al. 1986b, Bernard & Fenchel 1995, Fenchel & Bernard 1996), the oxygen penetration below the biofilms would be limited to depths of <1 mm, with >90% saturation typically depleted within the first 0.5 mm of sediment, if not within the biofilm completely (Fig. 3). This was in stark contrast to the OPD of the uncovered sediments adjacent to the biofilms (~2.2–3.6 mm; Table 1) and in unenriched sediments, where the OPD was up to ~3.9 mm.

An important consideration of this study was the coupling of the TOU measurements with DOU estimates in both biofilm-covered and uncovered sediments. In principle, the TOU in cohesive sediment is either greater than or equal to DOU, with the difference attributable to non-diffusive, biologically mediated uptake (Glud 2008). The exclusion of large fauna in this study resulted in diffusion being responsible for the TOU in unenriched or control sediments (Table 1). We found that sediments that received the lowest depositional load, 1.1 g C $m^{-2}$ $d^{-1}$, were able to maintain the same TOU:DOU ratio of ~1 despite the significant doubling of TOU rates from unenriched sediments (Fig. 2C). In these cores, the increase in DOU, which accommodated the rise in benthic oxygen demand, appeared to reach a 'plateau,' with DOU rates in uncovered sediments across all depositional loading groups stabilising at ~564 ± 111 µmol $m^{-2}$ $h^{-1}$ (Table 1). This pattern likely reflects the accumulation of organic matter on the sediment surface under higher depositional loads, with biofilm development over these concentrated deposits driving most of the TOU.

Estimates of DOU across biofilm-covered sediments were ~2 times higher than those rates estimated in the adjacent uncovered sediments (Table 1). Although a greater diffusive uptake rate across the biofilm is consistent with an increase in surface topography (Jørgensen & Des Marais 1990) and the high oxygen utilisation efficiency of sulfur-oxidising bacteria (Jørgensen 1982, Nelson et al. 1986a, Fenchel & Bernard 1995), the vertical insertion of the microelectrode through the biofilm may have also resulted in an overestimation of the 'covered' DOU (Glud et al. 1994). Regardless, even if we ignore a potential overestimation of DOU by 8–60% (Glud et al. 1994), diffusion alone was unable to explain the TOU when biofilms were present on the sediment surface (Table 1). Due to the exclusion of large fauna in this study, the decoupling of TOU and DOU correlating to the development of biofilms strongly suggests that the biofilms must have facilitated non-diffusive transport.

One potential mechanism for non-diffusive exchange in a biofilm is through vent-like structures, not too dissimilar to those visible in Fig. 2 (Fenchel & Glud 1998, Glud et al. 2004). Microsensor measurements in similar structures have displayed the upward transport of reduced metabolic solutes from beneath the biofilm, likely driven by advection. This process is presumed to be balanced by the downward movement of oxygen-rich overlying water through a convective counter-current (Fenchel & Glud 1998) or through larger basal openings at the edges of the biofilm structure (Glud et al. 2004). Such non-diffusive exchange is generated by the microbial community within the biofilms and is thought to be used to overcome the limitation of diffusion, enhancing the rates of reduced metabolic product oxidation and microbial respiration rates and increasing oxygen uptake rates by up to 40 times (Fenchel & Glud 1998).

Not only are these biofilms capable of shaping the subsurface oxygen structure and enhancing oxygen uptake (Jørgensen & Des Marais 1990, Fenchel & Glud 1998), but their chemolithotrophic production can act as an important food source for the benthic food web (Bernard & Fenchel 1995, Fenchel & Bernard 1995). That is, since some sulfur-oxidising bacteria grow via assimilatory reduction of $CO_2$ (Nelson & Jannasch 1983), the biofilm growth creates a carbon-rich system that may have otherwise been organically deplete. As such, the biofilm patchiness we observed in this study suggests that moderate organic farm deposits on organically deplete sediments can increase the structural heterogeneity of the larger-scale ecosystem and potentially promote grazing activity by 'new' food availability (Keeley et al. 2013).

While only 'patchy' covers of biofilms were observed after 1 wk of moderate organic loading, heavy depositional loads, similar to those simulated in the positive control group (~11.2 g C $m^{-2}$ $d^{-1}$; Keeley et al. 2013), can result in extensive biofilm coverage (Fig. 2). An expansion of biofilm coverage, becoming a cohesive 'mat' on the sediment surface, can result in the build-up of toxic solutes in surface sediments and has been associated with mass mortality of infauna that are unable to migrate from the covered area (Diaz & Rosenberg 1995). Moreover, extensive microbial mats can stabilise sediment surfaces against resuspension due to physical erosion (Grant 1988). Disturbances that do resuspend these mats can have significant impacts on benthic water quality from

benthic nutrient release, disrupted sulfur cycling, and the potential increased toxicity of the surrounding benthic system (Grant & Bathmann 1987), forming hypoxic 'dead zones' (Joyce 2000).

## 5. CONCLUSIONS

This study suggests that the deposition of excess organic material from farms limits the oxygenation of the sediments directly below the organic particles themselves — with little effect on adjacent sediments. This finding is not surprising, as these sediments, like those commonly found in offshore ecosystems, are cohesive, and porewater exchange is largely limited by rates of diffusion. The potential or unintended benefit of introducing a patchy footprint of waste deposition in an open-ocean environment, naturally deplete of organic matter, is that the surge in food availability may promote grazing activity and potentially increase the overall biodiversity of the seafloor environment. The observed patchiness of settlement and the associated formation of biofilms suggest that the accumulation of subsurface solutes will likely be limited. This limitation would come from an accelerated reoxygenation of reduced solutes along biofilm edges (Fenchel & Glud 1998) and the promotion of grazing activity (Keeley et al. 2012) that may prevent any 'large pulses' of reduced chemo-oxidative solutes that can lead to the formation of dead zones.

However, it is crucial to note that this study intentionally excluded large benthic grazers, a factor that could significantly alter the *in situ* dynamics of organic matter processing. Grazers such as macrofauna play an essential role in nutrient cycling, biofilm disruption, and the reworking of sediments, all of which could enhance oxygen exchange. Without these organisms, the sediment's ability to reoxygenate and regulate subsurface solutes may be underestimated.

It is also important to note that the introduction of organic material in this study maintained the particulate structure of the fish waste collected. This careful collection and addition of waste was intended to simulate the potential organic particle rain in open-ocean environments as has been seen inshore. We acknowledge and expect that the particulate waste that does reach the seafloor may be finer than what was deposited here; however, the potential for larger particles to settle and aggregate is an important consideration. Moreover, the development of bacterial biofilms indicates the efficient metabolic oxidation of diffuse sulfides within the sediment structure; however, while this creates a space between the oxic bottom waters and the potentially toxic dissolved sulfides, the bacterial expansion and maintenance of this thermodynamically narrow suboxic region (Sayama et al. 2005) could have a persistent footprint beyond the depositional event. More benthic monitoring is required to confirm whether this newly organic-rich sediment surface promotes the grazing activity suggested here.

*Acknowledgements.* The authors acknowledge the financial support of the Blue Economy Cooperative Research Centre, established and supported under the Australian Government's Cooperative Research Centres Program, grant number CRC-20180101, and New Zealand Seafood Innovations. Thanks are extended to those who assisted in the running of the experiment. Specifically, the boat crew on Kaharoa, NIWA, thank you for your company and incredible skills that were essential for the retrieval of the sediment cores. To S. Pether and A. Setiawan at NIWA Northland Research Centre, thank you for hosting M.N.S. for the duration of the experiment and providing staff support. A special thank you to S. Griffiths, M. Exton, G. Irvine, and D. Williams at NIWA Northland Research Centre for all their hard work during the setup, running, and breakdown of the incubation and waste collection systems. Thanks are also extended to participants for their consultation during the writing of the manuscript.

LITERATURE CITED

Berg P, Risgaard-Petersen N, Rysgaard S (1998) Interpretation of measured concentration profiles in sediment pore water. Limnol Oceanogr 43:1500–1510

Bernard C, Fenchel T (1995) Mats of colourless sulphur bacteria. II. Structure, composition of biota and successional patterns. Mar Ecol Prog Ser 128:171–179

Brackley HL, Blair NE, Trustrum NA, Carter L and others (2010) Dispersal and transformation of organic carbon across an episodic, high sediment discharge continental margin, Waipaoa Sedimentary System, New Zealand. Mar Geol 270:202–212

Diaz RJ, Rosenberg R (1995) Marine benthic hypoxia: a review of its ecological effects and the behavioural responses of benthic macrofauna. Oceanogr Mar Biol Annu Rev 33:245–303

Dyksma S, Bischof K, Fuchs BM, Hoffmann K and others (2016) Ubiquitous *Gammaproteobacteria* dominate dark carbon fixation in coastal sediments. ISME J 10:1939–1953

Fenchel T, Bernard C (1995) Mats of colourless sulphur bacteria. I. Major microbial processes. Mar Ecol Prog Ser 128:161–170

Fenchel T, Bernard C (1996) Behavioural responses in oxygen gradients of ciliates from microbial mats. Eur J Protistol 32:55–63

Fenchel T, Glud RN (1998) Veil architecture in a sulphide-oxidizing bacterium enhances countercurrent flux. Nature 394:367–369

Folk RL (1954) The distinction between grain size and mineral composition in sedimentary-rock nomenclature. J Geol 62:344–359

Fossing H, Gallardo VA, Jørgensen BB, Hüttel M and others

(1995) Concentration and transport of nitrate by the mat-forming sulphur bacterium *Thioploca*. Nature 374: 713–715

Glud RN (2008) Oxygen dynamics of marine sediments. Mar Biol Res 4:243–289

Glud RN, Gundersen JK, Revsbech NP, Jørgensen BB (1994) Effects on the benthic diffusive boundary layer imposed by microelectrodes. Limnol Oceanogr 39:462–467

Glud RN, Santegoeds CM, De Beer D, Kohls O, Ramsing NB (1998) Oxygen dynamics at the base of a biofilm studied with planar optodes. Aquat Microb Ecol 14:223–233

Glud RN, Rysgaard S, Fenchel T, Nielsen PH (2004) A conspicuous $H_2S$-oxidizing microbial mat from a high-latitude Arctic fjord (Young Sound, NE Greenland). Mar Biol 145:51–60

Grant J (1988) Intertidal bedforms, sediment transport, and stabilization by benthic microalgae. In: de Boer PL, van Gelder A, Nio SD (eds) Tide-influenced sedimentary environments and facies. Extended versions of papers presented at the Symposium on Classic Tidal Deposits, held August 1985 in Utrecht, Netherlands. Kluwer Academic, Dordrecht, p 499–510

Grant J, Bathmann UV (1987) Swept away: resuspension of bacterial mats regulates benthic–pelagic exchange of sulfur. Science 236:1472–1474

Hamoutene D, Salvo F, Donnet S, Dufour SC (2016) The usage of visual indicators in regulatory monitoring at hard-bottom finfish aquaculture sites in Newfoundland (Canada). Mar Pollut Bull 108:232–241

Holmer M, Wildish D, Hargrave BT (2005) Organic enrichment from marine finfish aquaculture and effects on sediment biogeochemical processes. In: Hargrave BT (ed) Environmental effects of marine finfish aquaculture. Handbook of environmental chemistry, Vol 5M. Springer, Berlin, p 181–206

Jørgensen BB (1982) Ecology of the bacteria of the sulphur cycle with special reference to anoxic–oxic interface environments. Philos Trans R Soc B 298:543–561

Jørgensen BB, Des Marais DJ (1990) The diffusive boundary layer of sediments: oxygen microgradients over a microbial mat. Limnol Oceanogr 35:1343–1355

Joyce S (2000) The dead zones: oxygen-starved coastal waters. Environ Health Perspect 108:A120–A125

Keeley NB, Forrest BM, Crawford C, MacLeod CK (2012) Exploiting salmon farm benthic enrichment gradients to evaluate the regional performance of biotic indices and environmental indicators. Ecol Indic 23:453–466

Keeley NB, Cromey CJ, Goodwin EO, Gibbs MT, Macleod CM (2013) Predictive depositional modelling (DEPOMOD) of the interactive effect of current flow and resuspension on ecological impacts beneath salmon farms. Aquacult Environ Interact 3:275–291

Kennedy P, Kennedy H, Papadimitriou S (2005) The effect of acidification on the determination of organic carbon, total nitrogen and their stable isotopic composition in algae and marine sediment. Rapid Commun Mass Spectrom 19:1063–1068

Middelburg JJ, Duarte CM, Gattuso JP (2005) Respiration in coastal benthic communities. In: del Giorgio PA, Williams PJB (eds) Respiration in aquatic ecosystems. Oxford University Press, Oxford, p 206–224

Møller MM, Nielsen LP, Jørgensen BB (1985) Oxygen responses and mat formation by *Beggiatoa* spp. Appl Environ Microbiol 50:373–382

Nelson DC, Jannasch HW (1983) Chemoautotrophic growth of a marine *Beggiatoa* in sulfide-gradient cultures. Arch Microbiol 136:262–269

Nelson DC, Jørgensen BB, Revsbech NP (1986a) Growth pattern and yield of a chemoautotrophic *Beggiatoa* sp. in oxygen-sulfide microgradients. Appl Environ Microbiol 52:225–233

Nelson DC, Revsbech NP, Jørgensen BB (1986b) Microoxic-anoxic niche of *Beggiatoa* spp.: microelectrode survey of marine and freshwater strains. Appl Environ Microbiol 52:161–168

Preisler A, De Beer D, Lichtschlag A, Lavik G, Boetius A, Jørgensen BB (2007) Biological and chemical sulfide oxidation in a *Beggiatoa* inhabited marine sediment. ISME J 1: 341–353

R Core Team (2023) R: a language and environment for statistical computing. R Foundation for Statistical Computing, Vienna

Riekenberg PM, Oakes JM, Eyre BD (2020) Shining light on priming in euphotic sediments: nutrient enrichment stimulates export of stored organic matter. Environ Sci Technol 54(18):11165–11172

Røy H, Huettel M, Jørgensen BB (2004) Transmission of oxygen concentration fluctuations through the diffusive boundary layer overlying aquatic sediments. Limnol Oceanogr 49:686–692

Sayama M, Risgaard-Petersen N, Nielsen LP, Fossing H, Christensen PB (2005) Impact of bacterial $NO_3^-$ transport on sediment biogeochemistry. Appl Environ Microbiol 71:7575–7577

Simone M, Grant J (2020) Visually-based alternatives to sediment environmental monitoring. Mar Pollut Bull 158: 111367

Valdemarsen T, Bannister RJ, Hansen PK, Holmer M, Ervik A (2012) Biogeochemical malfunctioning in sediments beneath a deep-water fish farm. Environ Pollut 170:15–25

Valdemarsen T, Hansen PK, Ervik A, Bannister RJ (2015) Impact of deep-water fish farms on benthic macrofauna communities under different hydrodynamic conditions. Mar Pollut Bull 101:776–783

Wieland A, de Beer D, van Dusschoten D, Damgaard LR, Kuehl M, van As H (2001) Fine-scale measurement of diffusivity in a microbial mat with NMR imaging. Limnol Oceanogr 46:248–259

*Editorial responsibility: Catriona MacLeod, Hobart, Tasmania, Australia*
*Reviewed by: F. Bravo and 2 anonymous referees*
*Submitted: May 23, 2024; Accepted: December 9, 2024*
*Proofs received from author(s): February 17, 2025*